Riparian hydraulic gradient and stream-groundwater exchange dynamics in steep headwater valleys

Thomas Voltz,[1] Michael Gooseff,[2,3] Adam S. Ward,[4] Kamini Singha,[5] Michael Fitzgerald,[6] and Thorsten Wagener[7]

Received 28 February 2012; revised 16 April 2013; accepted 19 April 2013.

[1] Patterns of riparian hydraulic gradients and stream-groundwater exchange in headwater catchments provide the hydrologic context for important ecological processes. Although the controls are relatively well understood, their dynamics during periods of hydrologic change is not. We investigate riparian hydraulic gradients over three different time scales in two steep, forested, headwater catchments in Oregon (WS01 and WS03) to determine the potential controls of reach-scale valley slope and cross-sectional valley geometry. Groundwater and stream stage data collected at high spatial and temporal resolutions over a period encompassing a 1.25 year storm and subsequent seasonal baseflow recession indicate that hydraulic gradients in both riparian aquifers exhibit strong persistence of down-valley dominance. Responses to rainfall do not support the simple conceptual models of increased riparian hydraulic gradient toward streams. Hydraulic gradient response in WS01 to both the seasonal baseflow recession and the storm suggested the potential for increased stream-groundwater exchange, but there was less evidence for this in WS03. Results from four constant-rate tracer injections in each stream showed a high baseline level of exchange overall, and both a slight seasonal increase (WS01) and slight decrease (WS03) in the riparian intrusion of tracer-labeled stream water as stream discharge receded. These results indicate that steep headwater valley floors host extensive stream water exchange and very little change in the water table gradients over 3 orders of magnitude of stream discharge.

Citation: Voltz, T., M. Gooseff, A. S. Ward, K. Singha, M. Fitzgerald, and T. Wagener (2013), Riparian hydraulic gradient and stream-groundwater exchange dynamics in steep headwater valleys, *J. Geophys. Res. Earth Surf.*, *118*, doi:10.1002/jgrf.20074.

1. Introduction

[2] Predictions of stream water and groundwater interactions are challenging to make (see *Sophocleous* [2002] for overview; *Woessner* [2000]) due to, for example, site-specific conditions, including temporal and spatial variability in hydraulic conductivity fields, head gradients, hydraulic boundary conditions adjacent to streams. Despite this recognition, several researchers have proposed models of hydrologic interactions between aquifers and streams as a function of basin topography. For example, *Larkin and Sharp* [1992] developed groundwater flow models of alluvial aquifers to determine the extent to which stream-groundwater exchanges were functions of channel and valley geomorphic form: stream sinuosity, slope, channel incision, width-to-depth ratio, and fluvial depositional system. They predicted that these factors influenced subsurface flow directions, namely magnitudes of "underflow" (down-valley subsurface flow) and "baseflow" (cross-valley subsurface flow). Underflow was shown to be the dominant of these two fluxes in steep valley floor settings, and baseflow, the dominant flux in lower-gradient valleys. These findings, however, were presented as static with no accounting for temporal dynamics. In this paper, we seek to understand how seasonal, storm-driven, and diel changes in down-valley and cross-valley riparian flow dynamics occur in two steep headwater basins. That is, given a fixed geomorphic template, we seek to determine whether the conceptual model of *Larkin and Sharp* [1992] holds over a range of discharge conditions.

[3] Stream-groundwater interactions occur at a range of spatial scales. Most headwater streams are net gaining streams, and it is therefore tempting to represent them by the simplified conceptual model in which lateral flowpaths from hillslopes drain toward the stream. Associated with

[1]University of Applied Sciences, Faculty of Civil Engineering/ Architecture, Division of Water Sciences, Dresden, Germany.
[2]Department of Civil and Environmental Engineering, Pennsylvania State University, University Park, Pennsylvania, USA.
[3]Now at Department of Civil and Environmental Engineering, Colorado State University, Fort Collins, Colorado, USA.
[4]Department of Geoscience, University of Iowa, Iowa City, Iowa, USA.
[5]Hydrologic Science and Engineering Program, Colorado School of Mines, Golden, Colorado, USA.
[6]NEON, Inc., Boulder, Colorado, USA.
[7]Department of Civil Engineering, University of Bristol, Bristol, UK.

Corresponding author: M. Gooseff, Department of Civil and Environmental Engineering, Pennsylvania State University, University Park, PA 16802, USA. (mgooseff@engr.psu.edu)

©2013. American Geophysical Union. All Rights Reserved.
2169-9003/13/10.1002/jgrf.20074

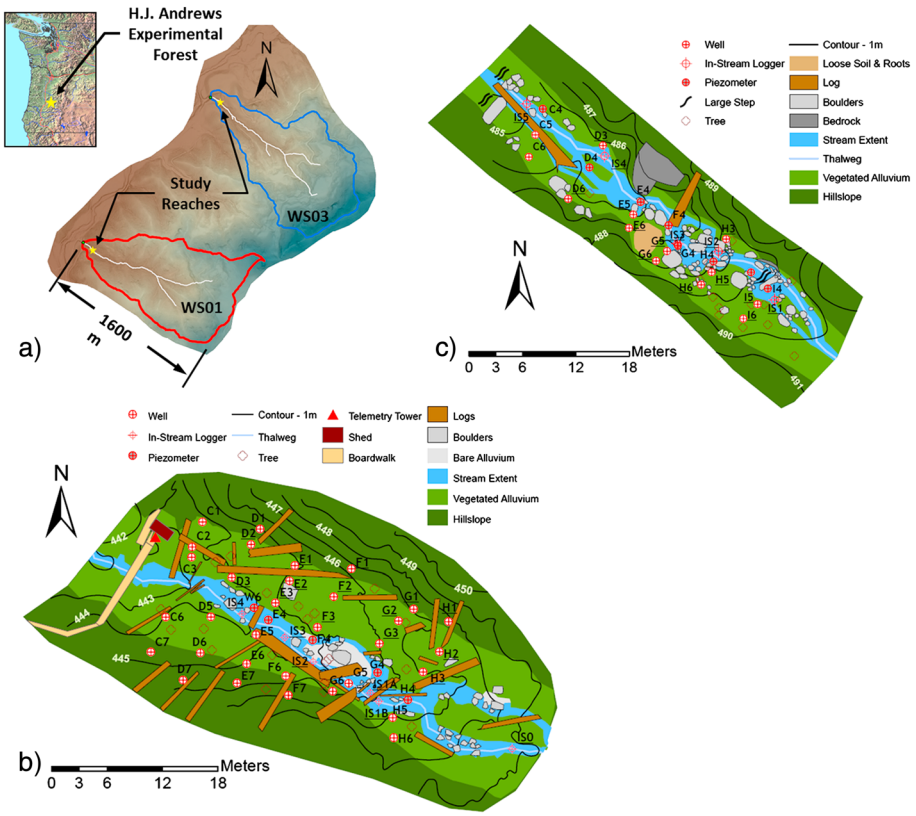

Figure 1. (a) General location map of the HJ Andrews Experimental Forest and two watersheds of interest, WS01, and WS03, derived from airborne LIDAR data, and valley floor segment maps of (b) WS01 and (c) WS03 including well network detail. Flow in both stream reaches is from lower right to upper left. The image of the Pacific Northwest region was taken from USGS Seamless Data Warehouse (unpublished data, 2012), available at http://seamless.usgs.gov/.

this simplified riparian hydrology conceptual model is the expectation of high water tables adjacent to the channel driving strong cross-valley hydraulic gradients toward the stream, i.e., the groundwater ridging hypothesis [*Sklash and Farvolden*, 1979]. However, even in net gaining streams, bi-directional exchange of stream water, in which some portion of the riparian zone accommodates stream water exchanging through the subsurface (and vice versa), occurs despite the expected steep head gradients from the riparian zone to the channel [*Payn et al.*, 2009; *Covino et al.*, 2011]. This suggests that head gradients around streams at high flow conditions must be spatially variable to accommodate exchange flows from the stream [*Wroblicky et al.*, 1998]. Thus, conceptual models of stream-groundwater interactions, such as that of hydrologic landscapes, which suggests that water tables generally follow surface topography, except very close to surface water bodies [*Winter*, 2001], require some refinement at the spatial scale of the valley floor.

[4] Stream-groundwater interactions must be understood in the context of riparian zone and/or valley-bottom hydrology, which has been identified as an important control on the efficacy of riparian zone biogeochemical cycling, and stream water quality [*Cirmo and McDonnell*, 1997]. For example, with respect to denitrification, riparian soils may host fairly consistent uptake rates [*Groffman et al.*, 1996] or demonstrate a stratified potential, where surface soils (approximately 20 cm or less) have much higher potential denitrification rates than deeper soils [*Burt et al.*, 1999]. In the latter case, water table elevation would influence how effective a riparian zone could be at removing nitrate. However, most hydrogeological conceptual models of the riparian zone as an intermediary between hillslopes and channels remain relatively simple. *Burt et al.* [2008] note that "the riparian zone is perhaps the most important element of the hydrological landscape given that it can decouple the linkage between the major landscape elements, hillslope and channel". Indeed, several studies have focused on riparian hydrology, linking hillslopes to channels [e.g., *Vidon and Hill*, 2004; *Duval and Hill*, 2006; *Jencso et al.*, 2009]. Left out of this perspective is the bi-directional exchange of stream and groundwater. This simplistically treats the riparian zone as a location that is grossly influenced by boundary head gradients, where the end members are the stream and hillslopes [*Duval and Hill*, 2006]. As such, the stream water-influenced parts of the valley floor are not quantified. As such, the biogeochemical, heat and energy processing of riparian and hyporheic zones, and the associated impacts on stream water quality are difficult to assess.

[5] Several studies have incorporated a conceptual model of varying lateral water tables as catchments wet (high water tables) and dry (low water tables) to explain stream water contributions to streams during periods of storm or baseflow recession. Water tables in headwater catchment hillslopes

Table 1. Physical Attributes of Study Watersheds and the Instrumented Stream Reaches

Physical Attribute	Watershed 1	Watershed 3
Whole Watershed		
Area[a] (hectares)	95.8	97.2
Aspect[b] (true north-azimuth)	290°36′ (WNW)	314°24′ (NW)
Elevation[c] above m.s.l.		
Maximum (m)	1018	1077
Minimum (m) [at flume]	432	472
Lee's Radiation Index[d]	41.9	36.5
Study Reach and Riparian Area		
Length (m) [along stream]	24	24
Width (m) [perpendicular to stream]	10	4
Mean Channel Slope (%)	11.9	13.8
Strahler Stream Order	2	2

[a]Calculated in ESRI ArcMap using 2010 1 m LIDAR.
[b]Data taken from *Rothacher et al*. [1967].
[c]Based on 2010 1 m LIDAR.
[d]Higher number indicates greater incident solar radiation.

and adjacent to streams have been observed to rise in response to storm events, promoting streamflow generation [e.g., *Dunne and Black*, 1970], and fall in response to seasonal baseflow recession [*Burt et al*., 2002]. *Bond et al*. [2002] propose that the water tables of riparian aquifers of steep headwater catchments in the western US will relax significantly during baseflow recession and, as a consequence, hyporheic exchange fluxes through the riparian aquifers will decrease with decreasing seasonal baseflow. *Wondzell et al*. [2010] suggest that this particular conceptual model linking riparian hydrology with stream-groundwater exchange in the same steep catchment is naïve in part because there is less riparian water table elevation decrease than is expected by the conceptual model put forward by *Bond et al*. [2002].

[6] The simple models of subsurface valley-bottom flow, especially those that are driven largely by surface topography [e.g., *Larkin and Sharp*, 1992], have not been thoroughly validated in the subsurface. These models are particularly attractive because surface topography data are relatively easy to obtain. An open question remains as to whether such models apply through periods of storm and baseflow recession. If so, then the conclusion is that the morphology of the channel, valley floor, and hillslopes (together) is the dominant control on the lateral hydrologic boundary conditions for the stream. In this paper we seek to investigate how the relative dominance of down-valley and cross-valley hydraulic gradients in headwater valleys change over various time scales, interpret these changes in the context of the reach-scale valley slope and cross-sectional valley geometry by comparing them to the corresponding land surface gradients, and assess how they might impact stream-groundwater interactions. We monitored riparian groundwater levels through a seasonal baseflow recession period (approximately 01 June–22 August 2010) in two headwater stream valleys in the HJ Andrews Experimental Forest, Oregon, USA. We focus our analyses of riparian hydraulic gradients on three different hydrologic conditions and time scales: (1) across seasonal baseflow recession (June to August), (2) in response to a storm that occurred at the beginning of baseflow recession, and (3) during diurnal discharge and water table fluctuations late in the baseflow recession period. We also assess the impact of seasonal baseflow recession on the extent of stream water intrusion into the riparian aquifers adjacent to these streams by performing salt tracer injections throughout. Based on the findings of *Wondzell* [2006], *Wondzell et al*. [2010] and *Ward et al*. [2012], we hypothesize that there will be little variation in the general direction of riparian hydraulic gradients throughout baseflow recession and across all three time scales across a wide range of hydrologic conditions due to the steep valley slope and narrow valley cross-section.

2. Site Description

[7] The two headwater valley segments used in this study are within watershed 1 (WS01; ~21 m instrumented length) and watershed 3 (WS03; ~25 m instrumented length) of the HJ Andrews Experimental Forest (HJA) in the western Cascade Mountains, Oregon, USA (Figure 1a). Both valleys are deeply dissected by their streams, with very steep hillslopes (> 50%) and high-gradient stream channels (≈ 15%) (Table 1). Valley-bottom riparian areas are narrow (≤ 10 m for WS03 and ≤ 20 m for WS01). The two stream reaches used in this study were previously instrumented with shallow wells and piezometers as reported by *Wondzell* [2006]. They are both

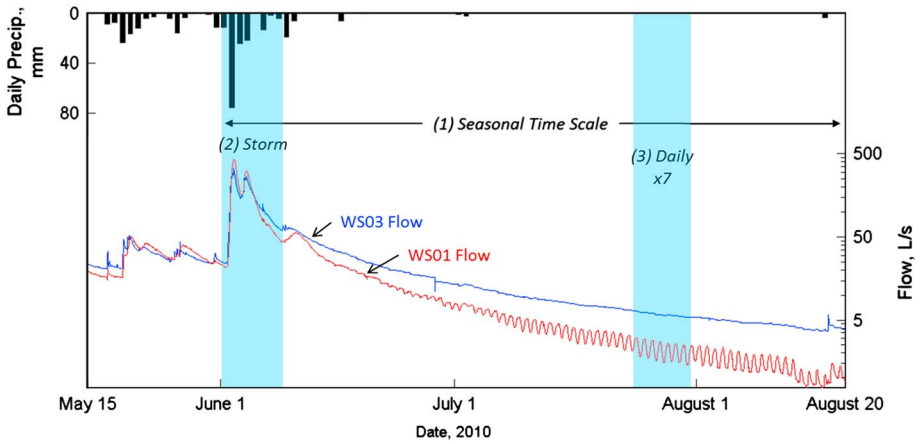

Figure 2. Hyetograph and hydrograph showing hydrologic conditions for the seasonal baseflow recession, and the time scales considered in our assessment. The daily timescale is shown for a typical 7 day period during baseflow recession.

Table 2. Down-Valley Gradient (DV), Cross-Valley Gradient (CV) and the Ratio of Cross- to Down-Valley Gradient (CDVR) Magnitudes of the Land Surface for All Triangular Elements Considered[a]

Watershed 1				Watershed 3			
Triangular Element	Land Surface Data			Triangular Element	Land Surface Data		
	DV Grad	CV Grad	CDVR		DV Grad	CV Grad	CDVR
NH1	0.13	−0.06	*−0.44*	NH1	0.29	0.71	2.40
NH2	0.13	0.38	2.93	NH2	0.12	−0.04	*−0.35*
NH3	0.09	−0.06	*−0.75*	NH3	0.11	0.78	7.19
NH4	0.16	0.29	1.81	NH4	0.05	0.31	6.43
NH5	0.13	0.30	2.31	NH5	0.20	0.34	1.70
NH6	0.08	0.17	2.15	NH6	0.19	0.18	*0.97*
NH7	0.16	0.13	*0.78*	NH7	0.21	0.11	*0.53*
NH8	0.17	0.14	*0.83*	**MEAN**	**0.17**	**0.34**	**2.70**
MEAN	**0.13**	**0.16**	**1.20**	SA1	0.20	0.21	1.08
MR1	0.14	−0.03	*−0.25*	SA2	0.21	0.22	1.02
MR1a	0.15	−0.06	*−0.38*	SA3	0.22	0.18	*0.82*
MR2	0.11	0.04	*0.33*	SA4	0.22	0.27	1.23
MR3	0.09	0.04	*0.46*	**MEAN**	**0.21**	**0.22**	**1.04**
MR4	0.08	0.02	*0.31*	TS1	0.02	0.12	5.69
MR5	0.08	0.02	*0.29*	TS2	0.16	−0.17	−1.05
MR6	0.14	0.19	1.34	TS3	0.23	−0.10	*−0.43*
MR7	0.22	0.17	*0.75*	TS4	0.20	−0.09	*−0.46*
MR8	0.15	0.08	*0.52*	TS5	0.08	0.16	2.15
MEAN	**0.13**	**0.05**	**0.38**	**MEAN**	**0.14**	**−0.02**	**1.18**
SA1	0.13	0.37	2.78				
SA2	0.13	0.38	3.02				
SA3	0.11	0.36	3.36				
SA4	0.22	0.24	1.11				
SA5	0.05	0.19	3.82				
SA6	0.16	0.06	*0.37*				
SA7	0.21	0.07	*0.35*				
MEAN	**0.14**	**0.24**	**2.12**				

[a]CDVRs between −1 and 1 indicate a down-valley flow preference, and CDVRs magnitudes > 1 indicate a stronger cross-valley than down-valley gradient. It is not particularly likely for down-valley gradient to have a value < 0, but the cross-valley gradient can certainly be positive or negative, indicating a direction toward left hand bank of the channel if positive, and the right hand bank of the channel if negative (see Figure 4). Zones are near hillslope (NH), middle riparian (MR), stream adjacent (SA), and through stream (TS).

located very close to the watershed outlets, within 100 m upstream of permanent flow-gauging stations.

[8] The HJA has a Mediterranean climate, with wet, mild winters and dry, cool summers [*Rothacher et al.*, 1967]. Snow packs form at lower elevations, but seldom last more than a few weeks. Most of the precipitation (~2300 mm annually) falls as rain from October to May [*Swanson and Jones*, 2002], resulting in a baseflow recession period that begins in mid- to late June and lasts until late August or September. The period of this study (2010) had a fairly typical seasonal baseflow recession (Figure 2).

[9] The surface geology of HJA is young, consisting of derivatives of volcanic lava, mud, or pyroclastic flows [*Swanson and James*, 1975]. The bedrock in WS01 and WS03 is dominated by breccias and tuffs deposited by the last volcanic activity during the Oligocene and lower Miocene epochs about 24 million years ago. These formations are readily weatherable, resulting in thick layers of unconsolidated, weathered rock on top of consolidated bedrock, and they lend themselves to extensive mass movements in the steep terrain found in WS01 and WS03.

[10] Soils in WS01 and WS03 are predominately shallow (1–2 m) with limited profile development and considerable gravel and cobbles, although these are often underlain by thick layers of unconsolidated, weathered parent material. Depth to relatively impermeable bedrock is not obvious, and in some locations may exceed 15 m. Although all soils found in WS01 and WS03 are texturally classified as loam and contain significant percentages of fines (> 20%), they tend to display massive, well-aggregated structure that contributes to high porosity (> 50% in all cases, up to 75%) and infiltration rates (about 500 cm/h, but variable) [*Rothacher et al.*, 1967; *Dyrness*, 1969].

2.1. Study Valley Segments

[11] In WS01, steep hillslopes outside of the riparian area give way to a much lower cross-valley-gradient floor (Figure 1b). The valley segment includes many large fallen trees that are decomposing, and several large boulders, concentrated in the stream channel. The stream spatial extent shown in Figure 1b reflects conditions in March 2010, towards the end of the wet season. The morphology of the stream in this reach with an average of 11.9% slope is a series of steps (many formed by downed trees), pools, and riffles. A number of deciduous trees (mostly red alder) have grown in the riparian zone.

[12] The valley-bottom segment of WS03 (Figure 1c) is narrower than that of WS01. Hence, the well/piezometer network was more limited than that in WS01. The two streams are otherwise morphologically similar, and like WS01 the stream in WS03 is a series of steps, riffles, and pools, and generally does not follow a well-defined channel. The riparian zone of WS03 contains only some young deciduous trees.

[13] We chose to divide the valley floors of both watersheds into different zones to group potentially similar groundwater responses. In WS01 we considered three zones: near

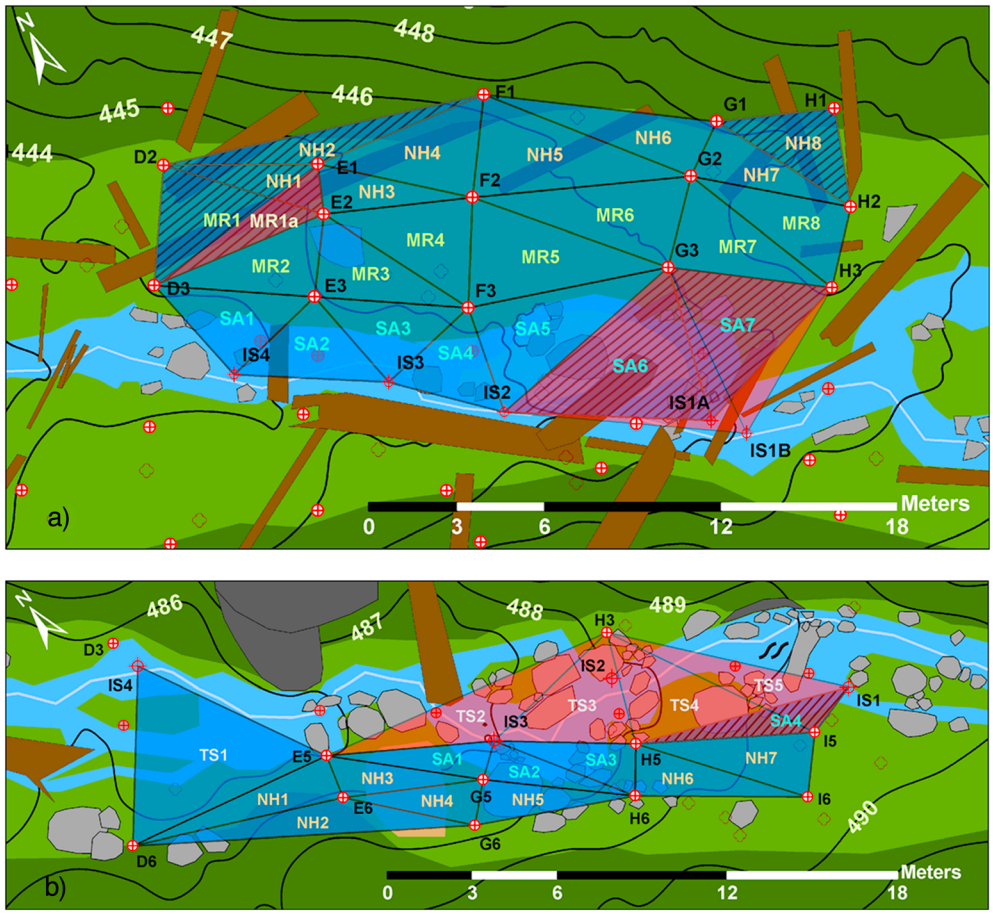

Figure 3. Riparian areas divided into near-hillslope (NH), middle-riparian (MR), stream-adjacent (SA), and through-stream (TS) zones for (a) WS01, and (b) WS03. Triangular elements with hatching denote gradient records that ended before the end of the season, and red-shaded elements are those that began part-way through the season, due to drying of wells.

hillslope (NH; ~5–8 m from shore line), middle riparian (MR; ~1–5 m from shore line), and stream-adjacent (SA; 0–1 m from shore line). In WS03 we considered: near hillslope (NH; ~1–4 m from shore line), stream adjacent (SA; 0–2 m from shore line), and through stream (TS; 0–2 m from shore lines). The ground surface topographic gradients, broken up into two vectors, cross-valley gradient, and down-valley gradient, are reported in Table 2.

3. Methods

3.1. Monitoring Water Table Elevations

[14] To quantify the spatial and temporal patterns of both the down- and cross-valley riparian hydraulic gradients, we collected groundwater level measurements at a high spatial density in the existing shallow well/piezometer networks (described in *Kasahara and Wondzell* [2003]; *Wondzell* [2006]) in the summer of 1997 (Figures 1b and 1c). Well casings were constructed from 3.175 cm diameter PVC pipe, screened over the bottom 50 cm by drilling 0.32 cm diameter holes at a density of about 0.25 holes/cm^2. Wells were driven in directly by hand and penetrate to depths between 0.75 and 1.5 m below the ground surface. Since their installation 13 years ago, some wells were destroyed or rendered unusable, leaving a network of 32 riparian monitoring wells and 13 piezometers in WS01 and WS03, respectively, available during our 2010 summer field season. We collected water table data from 1 June to 20 August 2010.

[15] The wells instrumented with water level loggers are shown with underlined labels in Figure 1b (WS01) and Figure 1c (WS03). Availability of loggers did not match the total number of wells and piezometers, so we chose to focus most deployments on a single side of the stream. In-stream loggers were generally placed in pools in line with well transects. Some of the wells and one in-stream pool went dry during the summer, ending some water level records before the end of the field season (e.g., H1 and D2 in WS01), and requiring relocation of one in-stream logger (IS1 in WS01). In WS03, in one location the monitored area extended beyond the stream channel to well H3, the record for which begins after 20 June 2010. Otherwise, all loggers recorded data uninterrupted for the entire field season.

[16] We used three types of pressure data loggers to monitor water levels in wells and the stream: HOBO model U20-001-04 (range 0–4 m, accuracy ± 3 mm, resolution 1.4 mm) by Onset, Levelogger Gold model (range 0–5 m, accuracy of 2.5 mm, resolution 0.05 mm) by Solinst, and CTD Diver (range 0–30 m, accuracy ± 30 mm, resolution 6 mm) by Van Essen Instruments. One barometric logger located at an above-ground fully shaded location in WS01 was

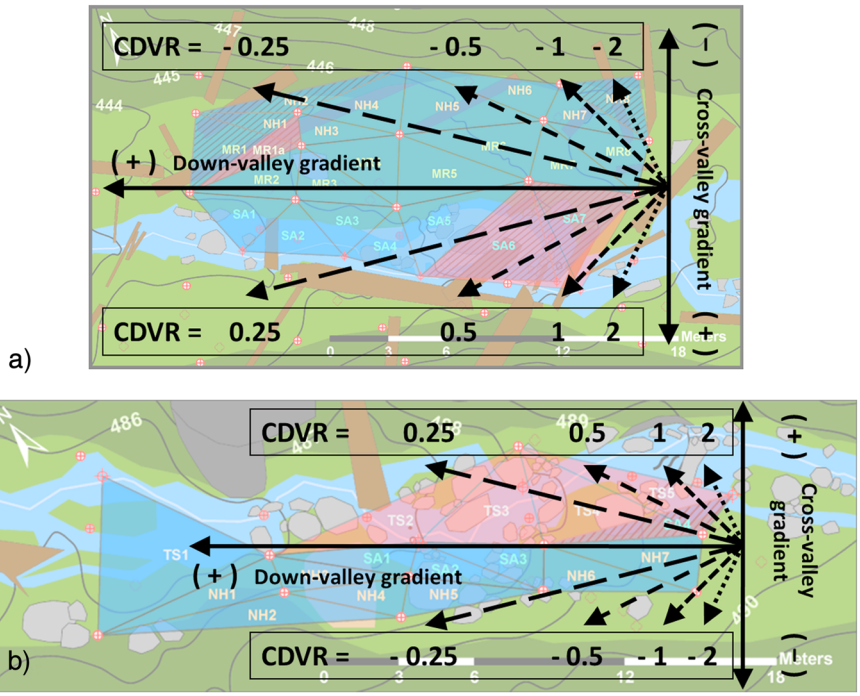

Figure 4. Illustration of the physical meaning of different hypothetical values of the cross- to down-valley ratio (CDVR), for (a) WS01 and (b) WS03. Note that the cross-valley sign convention for WS03 is opposite that of WS01, so that in both cases, a positive CDVR indicates a gradient directed towards the stream channel.

used for compensating records from both watersheds. We also used capacitance rod water level loggers (WT-1000 and WT-250, TruTrack; ranges of 1000 mm and 250 mm, respectively; accuracy of ± 10 mm and ± 2.5 mm, respectively; resolution of 1 mm for both). All measurements were adjusted for water temperature changes and all loggers were calibrated prior to deployment. All water level loggers used in the study recorded data at a temporal resolution of 5 min. We made repeated checks of depth to water surface throughout the summer in each well so that we could correct time series records if needed. In doing so, this helped us overcome potential issues related to different accuracies. Resolution differences remain, which we expect were most influential during late summer analyses of water table elevations.

3.1.1. Analysis of Water Table Data

[17] Analysis of hydraulic gradients was completed using a linear interpolation on triangular planes generated by a Delaunay triangulation of all points in the monitoring network where phreatic water elevation was recorded. We used triangular planes defined by neighboring observation locations (Figure 3). Cross-valley and down-valley directional vectors were defined and calculated as perpendicular and parallel to the general down-valley axis of each study reach, respectively (Figure 4). After calculating these directional vectors (dH/dx and dH/dy, where H is head, x is the down-valley direction, and y is the cross-valley direction), we calculated cross- to down-valley vector ratios (CDVRs):

$$CDVR = \frac{dH/dy}{dH/dx} \quad (1)$$

[18] We interpret CDVRs with magnitudes of < 1 to indicate a down-valley flow preference (i.e., $dH/dx > dH/dy$), and CDVRs > 1 indicate a stronger cross-valley than down-valley gradient. It is not particularly likely for dH/dx to have a value < 0, but dH/dy can certainly be positive or negative, indicating a direction toward left hand bank of the channel if positive, and the right hand bank of the channel if negative (see Figure 4). It was hypothesized that due to the steep down-valley topographic gradient and narrow headwater valleys, the magnitudes of the hydraulic CDVRs would be predominantly less than 1 throughout the baseflow recession, indicating a consistent dominance of down-valley hydraulic gradients at both high and low baseflow conditions. We have also calculated down-valley and cross-valley gradients and CDVRs for the riparian surface topography, based on topographic surveys of well locations (accuracy of ~1 cm). This approach allows us to compute the static topographic gradients in the same manner that the dynamic hydraulic gradients are computed (i.e., among the same three points, which are the locations of the wells bounding the triangular analysis element).

3.2. Constant-Rate Salt Tracer Injections

[19] To assess the influence of changing riparian hydraulic gradients on stream-groundwater exchange, we conducted a series of continuous 48 h constant-rate stream tracer injections coupled with frequent measurement of fluid electrical conductivity (EC) in the networks of wells and piezometers. More detail and further analyses can be found in the companion study by *Ward et al.* [2012]. We injected a dissolved high-concentration NaCl solution into the stream to trace the movement of stream water into the riparian aquifer. The goal of each injection was to raise the EC of the receiving stream water 100 µS/cm above the background, which was about 40 µS/cm at the start of the season,

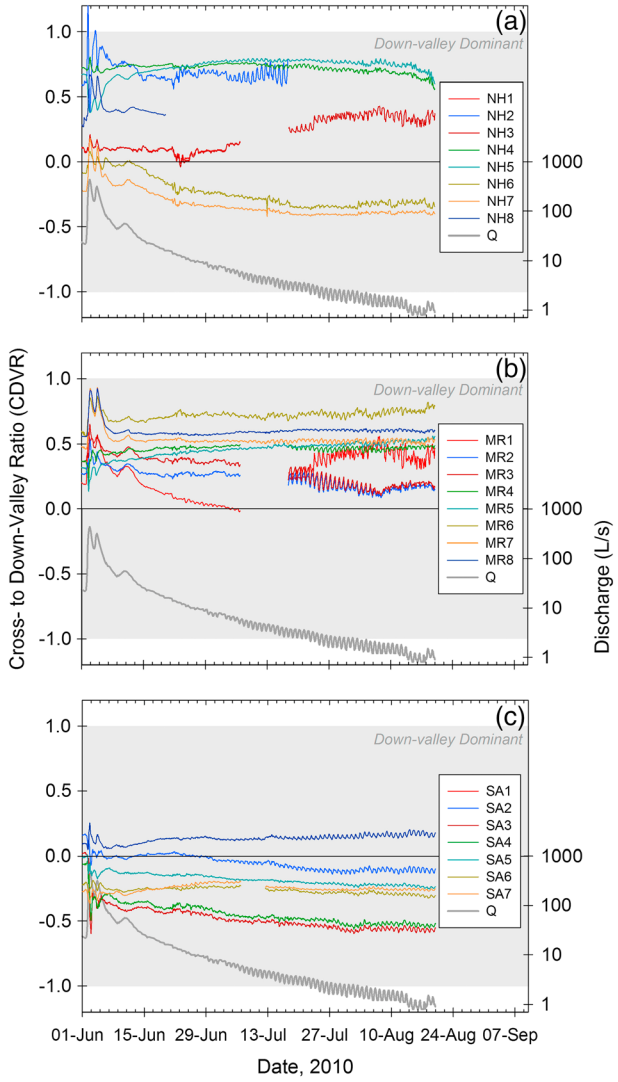

Figure 5. WS01 cross- to down-valley hydraulic gradient ratio (CDVR) for the entire field season, for (a) the near hillslope zone, (b) the middle riparian zone, and (c) the stream adjacent zone. The grey band indicates the region of down-valley dominance (i.e., $|CDVR| < 1$).

increasing to about 55 µS/cm at the end of the field season. Based on flow estimates from gauging stations located about 75 m downstream of each study segment, an appropriate mass of salt was dissolved in stream water and pumped continuously into the stream for 48 h, starting and ending at approximately 13:00. Injection locations in WS01 and WS03 were located about 40 m upstream of the upstream end of the study segments, allowing sufficient channel distance for complete mixing in the stream (verified through separate testing in which EC values were measured within stream cross sections and along the length of each study reach). Injections were completed a minimum of 2 weeks apart to ensure that EC in wells and the stream returned to a background condition so that the tail of one injection's tracer breakthrough curve did not interfere with the rising limb of the next.

[20] During and after stream tracer injections, the EC (temperature compensated) of the stream water was measured at 30 s intervals by Campbell Scientific CS547A EC probes, connected to Campbell CR-1000 data loggers. Fluid EC was measured in all water-bearing wells using a hand-held EC probe (YSI EC 300, range of 0–500 µS/cm, accuracy ± [1% of reading + 2 µS/cm], resolution 0.1 µS/cm). All readings were temperature compensated and taken following the evacuation of approximately one well volume of water to compensate for possible lack of rapid flow through wells and to achieve a more representative reading of the EC in the groundwater surrounding the well. Measurements (combination of all individual well readings) of EC across both monitoring networks were carried out at high frequency (20–30 min) during the few hours immediately following the start and end of the injection and every 3 h otherwise during and for several days after the injection. To gauge the relative penetration of salt tracer into the

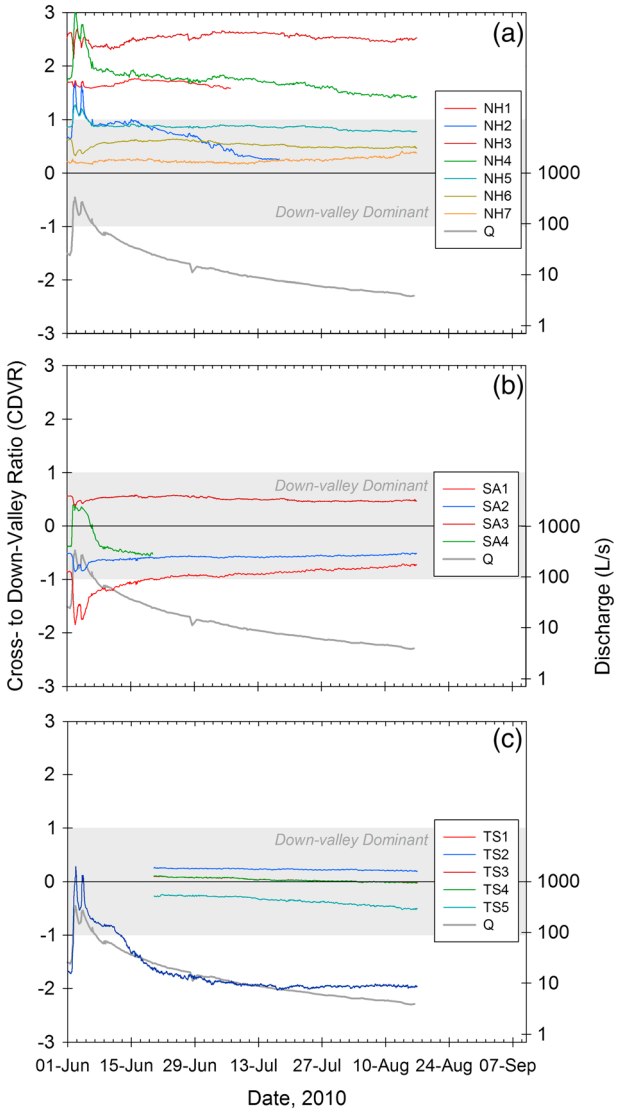

Figure 6. WS03 cross- to down-valley hydraulic gradient ratio (CDVR) for the entire field season, for (a) the near-hillslope zone, (b) the stream-adjacent zone, and (c) the through-stream zone. The grey band indicates the region of down-valley dominance (i.e., where $|CDVR| < 1$). Tick marks are displayed at 00:00 on the day labeled.

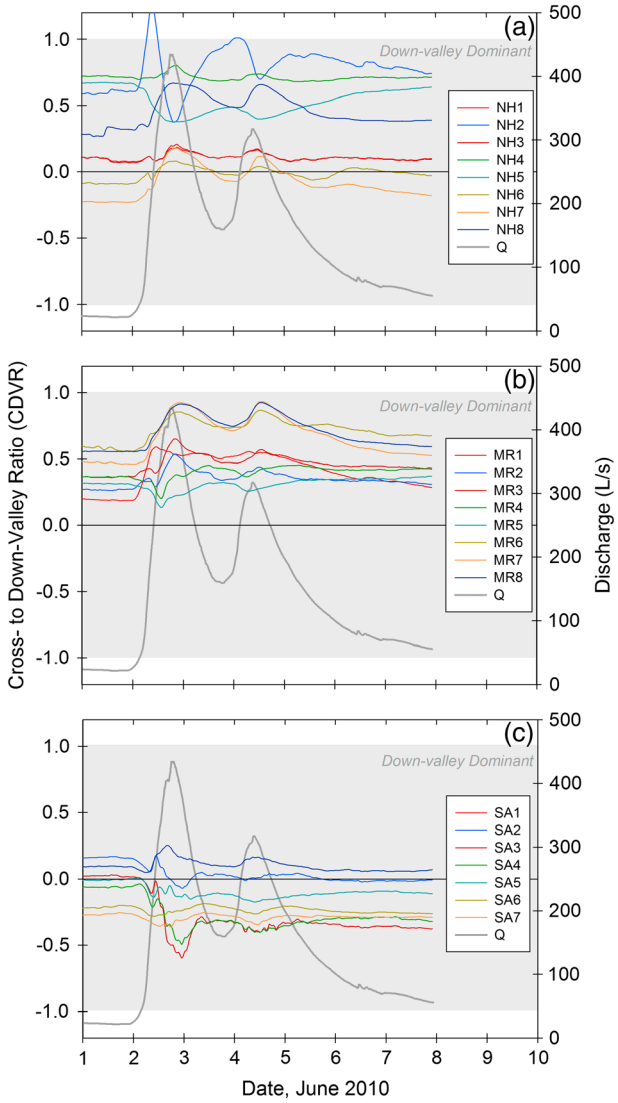

Figure 7. WS01 cross- to down-valley hydraulic gradient ratio (CDVR) for the 1–8 June storm period, for (a) the near-hillslope zones, (b) the middle riparian zones, and (c) the stream adjacent zones. The grey band indicates the region of down-valley dominance (i.e., $|CDVR| < 1$). Tick marks are displayed at 00:00 on the day labeled.

riparian aquifers through baseflow recession, we assessed the spatial pattern of relative changes in EC in the observation wells at the same point in time from the start of each injection. In WS01, this point was at 48 h, just before the injection pump was shut off. In WS03, 35 h was used, because of a pump malfunction toward the end of the first 48 h injection, resulting in rapid changes in both stream and riparian EC that would have impaired our ability to make comparisons between injections.

4. Results

4.1. Seasonal Hydraulic Gradient Dynamics

4.1.1. WS01

[21] The WS01 hydraulic CDVR time series for the entire field season reveals substantial variation in the behavior of each triangular element (Figure 5). Throughout the season only one hydraulic CDVR in any of the three zones (near hillslope [NH], middle riparian [MR], and stream adjacent [SA]) exceeded a magnitude of 1, indicating that at all times, hydraulic gradients were down-valley dominant. A majority of hydraulic CDVRs had a magnitude of 0.5 or less, particularly in the SA zone. All but one of the seven CDVRs in the SA zone were negative for the majority of the season and ultimately trended towards a more negative value (i.e., became more cross-valley away from the stream than down-valley in orientation—see Figure 4). However, the average CDVR of the surface topography in WS01 is 1.20 for the NH zone, 0.38 for the MR zone, and 2.12 for the SA zone (Table 2). In the NH zone, all hydraulic CDVRs have magnitudes of < 1 (except during the storm), yet, only half of these elements have topographic CDVRs with magnitudes of < 1. In the MR zone, all elements have hydraulic CDVRs that are between 0 and 1 throughout the summer (except MR7 for a few days at the end of its record), and all but one element (MR6) also have topographic gradients that range from 0 to 1. In the SA zone, all hydraulic CDVR magnitudes range between 0 and 1, but five of the seven elements have topographic CDVRs with magnitudes > 1. Thus, the hydraulic gradients are not well-aligned with the surface topography at the scale of a few meters within the riparian zone. A few of the hydraulic CDVRs (namely NH6, NH7, and SA2) crossed the zero axis of the plot during the storm, and then returned to the values closer to which they began. This indicates that some hydraulic gradients responded to the storm by rotating across the down-valley axis, but at most other times and at more prevalent lower flows favor one cross-valley direction over the other. Some hydraulic gradients (e.g., NH3, MR6, SA2, SA3, SA4, and SA5) responded to the storm by increasing cross-valley magnitude towards the stream, and then had the same tendency over the season, even as stream flow continued to recede. Others responded as predicted by the simplified riparian hydrology conceptual model described earlier (NH6, NH7, and MR1), increasing cross-valley magnitude in one direction during the storm, and then relaxing toward the down-valley direction as flow decreased through the season. A number of hydraulic gradients (NH2, NH3, MR1a, MR2, SA1, and SA2) showed diurnal fluctuations in CDVR after mid-July (Figure 5). Most interesting was the tendency for most of the CDVRs in the SA zone and some in the NH zone to gradually turn away from the stream as the season progressed, as it may have implications for changing patterns of stream-groundwater exchange.

4.1.2. WS03

[22] Similar to the record in WS01, streamflow receded substantially from June to August 2010 in WS03, however, there was not a prominent signature of diurnal streamflow fluctuation in WS03 (Figure 2). In the riparian aquifer of WS03, the CDVR for four hydraulic gradients (NH1, NH3, NH4, and TS1) always exceeded an absolute value of 1, nearly approaching 3 during the storm, while three others (NH2, NH5, and SA1) reached absolute values substantially greater than 1 during the storm before returning to the condition of down-valley dominance (Figure 6). This tendency is in contrast to the patterns observed in WS01 and is associated with the steeper riparian side slopes in WS03, particularly in the lower part of the valley segment

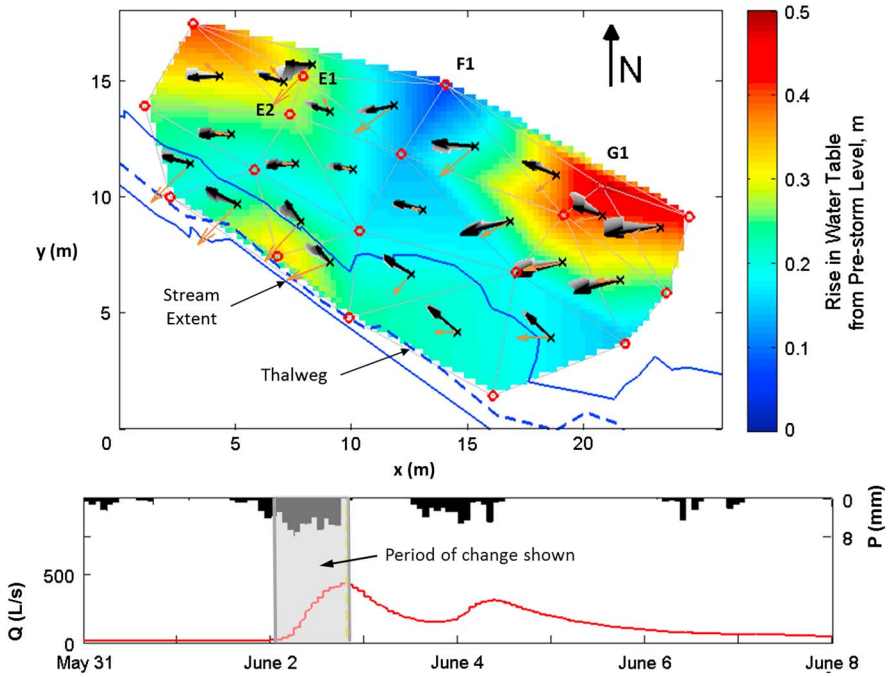

Figure 8. Time-lapsed image of the riparian hydraulic gradient storm response in WS01. Red circles indicate locations of water level measurement. Hydraulic gradient arrows (originating at x's) are plotted such that the arrow color transitions from light grey to black as time progresses over the storm response period. Brown arrows show the surface topographic gradients at the centroid of each element. The colored background indicates the rise in water level from the pre-storm level, to show how water levels rose to produce the observed gradient changes. Flow is from bottom right to top left. Tick marks are displayed at 00:00 on the day labeled. Hydrograph (Q) in red and hyetograph (P) in black are presented in the bottom panel.

(note the contours in Figure 1c and the topographic gradients reported in Table 2). Almost all zones also showed hydraulic CDVRs that do not vary much throughout the season, and with the exception of NH7 and TS5, they all shared a tendency to rotate slightly towards the down-valley axis. Thus, there appeared to be a minor "straightening out" of gradients occurring over the season. Most hydraulic gradients responded to seasonal declining flow by tending toward the direction opposite the way they responded to the storm, but NH3 (from about 8 June to 5 July) and NH6 showed the same general trajectory of response to both the storm and the ensuing seasonal dry period, although short-term (i.e., daily) fluctuations were dissimilar. All hydraulic gradients in the more distant NH zone showed a positive CDVR, pointing towards the stream, while three of the four gradients in the SA zone had primarily negative CDVRs, pointing away from the stream. The gradient of SA4 rotated across the down-valley axis towards the stream solely in response to the storm, and then returned to its more common condition of pointing away from the stream. With the exception of TS1, all of the CDVRs within the through-stream zone were close to zero, indicating a strong down-valley dominance. Topographic gradients in WS03 were variable, and topographic CDVRs range from −1.05 to 6.43 (Table 2). Six of the 16 elements in WS03 had topographic CDVRs with magnitudes < 1, yet 10 of the hydraulic CDVRs have consistent magnitudes of 1 or less. Thus, topography and hydraulic gradients are substantially different across the WS03 riparian zone.

4.2. Hydraulic Gradient Dynamics During a Storm

[23] Responses of the riparian hydraulic gradients to the storm were assessed during the first 8 days of June 2010, when two consecutive large rainfall events delivered about 13 cm of rain (Figure 2). The simple riparian hydrology conceptual model predicts that the magnitude of cross-valley hydraulic gradients should increase.

4.2.1. WS01

[24] Many gradients in the NH (6 of 8) and MR (6 of 8) zones of WS01 fit this model and show positive increases in CDVR (towards the stream), but only 1 of 7 in the SA zone exhibits this behavior (SA1) (Figure 7). All other hydraulic gradients showed the opposite effect, either diminishing the cross-valley component angled towards the stream (e.g., NH2, and NH5) or amplifying the cross-valley component already angled away from the stream (e.g., SA3–6). Moreover, only one hydraulic gradient (NH2) ever leaves the state of down-valley dominance during the storm, and the majority of CDVRs remained below 0.75 even at the storm peaks. So, even with variable responses observed through time, down-valley hydraulic gradient was always greater than the cross-valley gradient. The diversity of response observed throughout the WS01 riparian zone, with some water levels rising high and others rising hardly at all, is demonstrated during the initial rise of streamflow (Figure 8). It is difficult to attribute this variability of response to topographic features (e.g., local hillslope swales). For instance, it is unclear why well F1 showed almost no rise, and well G1, 7 m up-valley rose almost 0.5 m despite similar

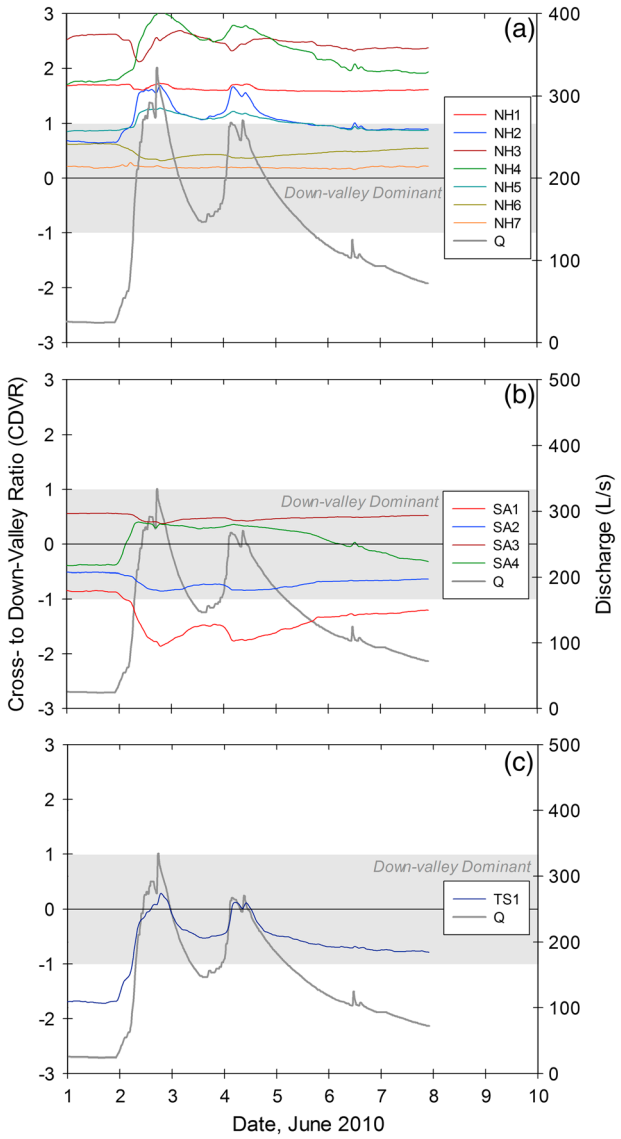

Figure 9. WS03 cross- to down-valley gradient ratio (CDVR) for the 1–8 June storm period for (a) the near-hillslope zone, (b) the stream-adjacent zone, and (c) the through-stream zone. The grey band indicates the region of down-valley dominance (i.e., where |CDVR| < 1). Tick marks are displayed at 00:00 on the day labeled.

hillslope gradients (Figure 1b). This difference at G1 might be due to boundary conditions of a small secondary channel that curves toward the main channel just upstream of the study reach. Most interesting from the perspective of stream-groundwater exchange is that several of the hydraulic gradients in the stream-adjacent zone turned farthest away from the stream at the peak of flow, while the other gradients in this zone did not change (Figure 8). This result suggests that, perhaps despite the hydraulic gradients in the NH and MR zones turning towards the stream, more stream water is driven into the riparian subsurface in response to rainfall events. This is contrary to what conventional conceptual models would predict, namely water tables increasing substantially in the riparian zone creating an increasing gradient toward the stream (i.e., *Dunne and Black* [1970], and the groundwater ridging hypothesis of *Gillham* [1984]). Further, the persistent down-valley dominance in all gradients is related to the steep headwater streams in general, in that even during substantial storm events most subsurface flow occurs parallel or at otherwise oblique angles to the stream, not directly towards the stream. Overall, most gradients in WS01 showed substantially larger changes in response to the storm than to the seasonal flow recession, although there were exceptions (NH3, NH6, NH7, and MR1). All hydraulic gradients exhibited down-valley dominance, to the greatest extent in the SA and MR zones. In most of the NH elements and all of the SA zones, hydraulic gradients during this storm response pointed more \downstream than the topographic gradients (Figure 8). However, in the MR zone, a mix of responses, but most ranges of hydraulic gradients were either very similar to topographic gradients or more down-valley oriented than the topographic gradients.

4.2.2. WS03

[25] In response to the early June 2010 storm, the time series of CDVR for WS03 (Figure 9) showed similar behavior to that of WS01, but with a greater tendency for stronger responses in the cross-valley direction, potentially due to the steeper cross-valley riparian slopes in much of the riparian area. As with WS01, most gradients in the NH zone showed positively increasing CDVR (reaching values between 1 and 3) in response to the storm, turning toward the stream, except for NH6, which showed the opposite behavior, and NH7, which showed almost no response to the storm (Figure 9). All NH zone gradients maintained a positive CDVR during and after the storm. In the MR zone, three of four gradients showed decreasing CDVR in response to the storm peaks. One (SA3) simply showed a less positive CDVR, but two (SA1 and SA2) began negative and became increasingly so, turning even further away from the stream. The fourth gradient (SA4) began with a negative CDVR and turned across the down-valley axis to have a cross-valley component pointing towards the stream during the storm peaks. The small-magnitude gradient TS1 showed a response analogous to that of SA4, beginning with a negative CDVR and just crossing the down-valley axis into the positive CDVR region, angling towards the stream. During the rise in streamflow, it is notable that there was a substantial decrease in total gradient magnitude of NH1 and NH3, caused by the relatively large rise at well E5 (Figure 10) (this result is not evident in the CDVR plots). The greatest changes during this initial storm response were the large, opposing gradients observed between NH4 and NH5, and between SA1 and SA2 (centered on well G5). The opposing tendencies of these gradients became intensified during the storm, in part due to the virtually negligible response shown by the water level in well G5. Elsewhere in the WS03 riparian area, some of the gradient responses (e.g., SA3) imply that more stream water has the potential to enter the subsurface (CDVRs indicate gradients turning away from the stream), and others (e.g., SA4) imply the opposite (CDVRs indicate gradients turn toward the stream). Further, similar to WS01, in eight of 11 elements, hydraulic gradients ranged in a more down valley direction than the topographic gradients (Figure 10).

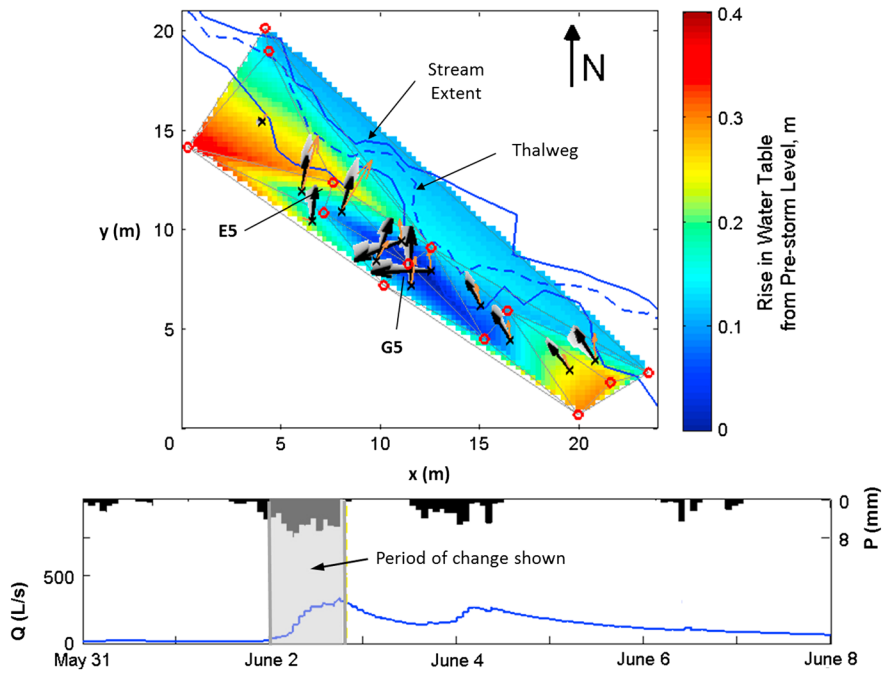

Figure 10. Time-lapsed image of the riparian hydraulic gradient storm response in WS03. Red circles indicate locations of water level measurement. Hydraulic gradient arrows (originating at x's) are plotted such that the arrow color transitions from light grey to black as time progresses over the storm response period. Brown arrows show the surface topographic gradients at the centroid of each element. The colored background indicates the rise in water level from the pre-storm level, to show how water levels rose to produce the observed gradient changes. Flow is from bottom right to top left. Tick marks are displayed at 00:00 on the day labeled. Hydrograph (Q) in blue and hyetograph (P) in black are presented in the bottom panel.

4.3. Hydraulic Gradient Dynamics Due To Diurnal Fluctuations

4.3.1. WS01

[26] Late in the baseflow recession period, diurnal fluctuations of streamflow were observed in WS01 (Figure 2), as are diurnal fluctuations of water tables in the riparian aquifer (Figure 11). These fluctuations occur due to the daily cycle of evapotranspiration from the watershed [*Wondzell et al*., 2010]. The effect of the diurnal water table fluctuations on stream discharge (and stage) was clearly identifiable, but the response of the hydraulic gradients was overall relatively slight. However, most gradients exhibited some diurnal fluctuation in CDVR, and the three gradients adjacent to wells E1 and E2 (MR1, MR2, and MR3) showed a strong response (especially at E2), compared to those observed in other zones. The hydraulic gradient in MR1 turned towards the stream as the flow and groundwater levels fall during the afternoon, trending the other direction at night. The MR1 hydraulic gradient also displays what appears to be a separation of signals from early in this week to later in the week, as the pattern of 1 peak per day changes to two peaks per day (Figure 11b). All other elements displayed the opposite behavior. As these locations are further removed from the stream, however, their effects are often obscured or blocked by those located nearer the stream, hence, they are less important to the question of whether diurnal fluctuations play a role in stream-groundwater exchange. In the SA zone, most CDVRs exhibited diurnal fluctuations (Figure 11c), typically reaching the most positive CDVR value shortly after the minimum flow and water table level. No fluctuations were great enough to cause a gradient to rotate across the down-valley axis (i.e., no CDVR changes sign throughout the course of a day, at least during the period presented), which would seem to be a necessary precursor to the potential for such short-timescale exchange patterns.

4.3.2. WS03

[27] A slight diurnal fluctuation of streamflow is also observed in WS03 (Figure 12), and the riparian CDVR response is negligible. Unlike the obvious fluctuations in flow seen in WS01, stream discharge in WS03 appears to gradually step down. Hence, there do not seem to be any diurnal fluctuations in the CDVRs of WS03 riparian gradients that could significantly affect movement of water through the valley floor aquifer on a diurnal time scale. WS03 has a comparable forest cover and size to WS01, but the evapotranspiration signal from the broader watershed is not as clearly linked to this stream as it is in WS01.

4.4. Stream Water Exchange With Riparian Zone Through Baseflow Recession

[28] To quantify changes in tracer penetration into the aquifer during baseflow recession, we compared temporal snapshots of the relative changes in EC in the observation well network between 0 and 48 h (for WS01) or 35 h (for WS03) after each injection began. The percent changes in the observation wells were normalized against those of the stream (which were essentially identical and set to a value of "1" in the figures) to give a sense of how far the salt-labeled stream water intruded into the riparian

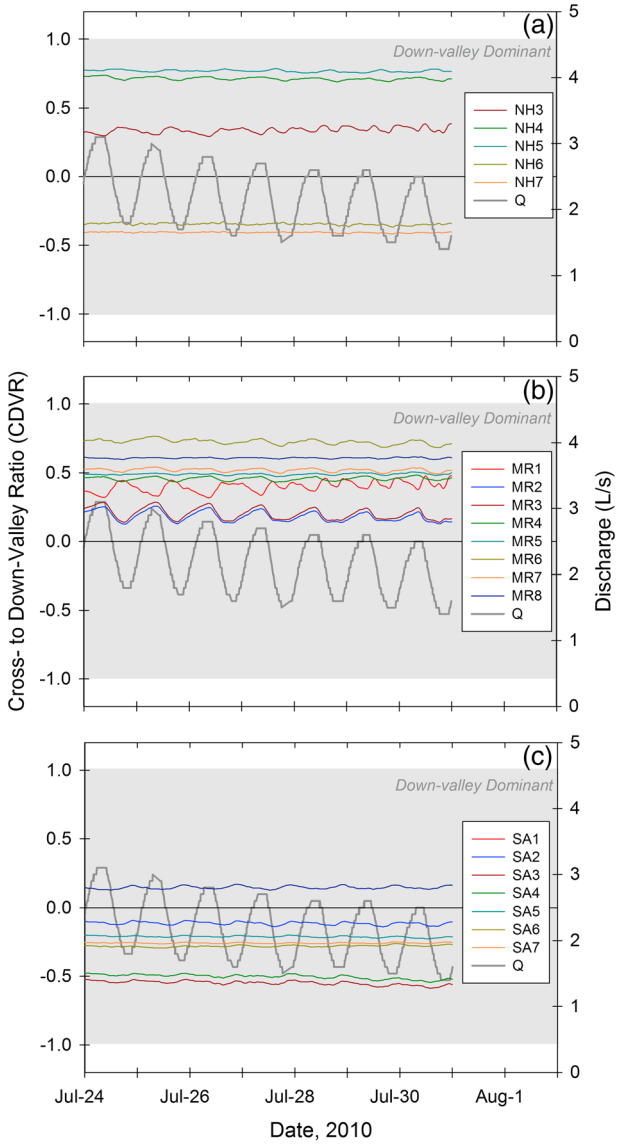

Figure 11. WS01 cross- to down-valley hydraulic gradient ratio (CDVR) for the period from 24 to 31 July for (a) the near hillslope zone, (b) the middle riparian zone, and (c) the stream adjacent zone. Tick marks are displayed at 00:00 on the day labeled.

aquifers. A more detailed interpretation of the tracer test data is given in the companion study by *Ward et al.* [2012].

4.4.1. WS01

[29] The increasing intrusion of salt-labeled stream water in the riparian aquifer of WS01 is readily apparent throughout the baseflow recession period (Figure 13). The change is most obvious between the first two injections, where salt-labeled stream water makes a large advance into the middle riparian area such that only three of wells, F1, E1, and D2, display relative EC changes are below 0.25. Steadily advancing intrusion can also be seen in the near-stream wells E3 and D3 from each injection to the next. Intrusion of stream water was extensive at the upstream-most transect of wells, despite being located as distant from the main channel (Thalweg) as most other transects. This may be evidence of the influence of the side channel above the study reach, which is forced to turn back towards the main channel just upstream of these transects, influencing subsurface movement of water. This explanation might also account for the lower EC observed in wells just downstream, since the hydraulic gradients calculated for that area would seem to send water on a flow path back to the stream. The gradual turning of the near-stream hydraulic gradients away from the stream throughout the baseflow recession season is consistent with the increased salt intrusion. The apparent slackening in tracer intrusion from the second to third injection

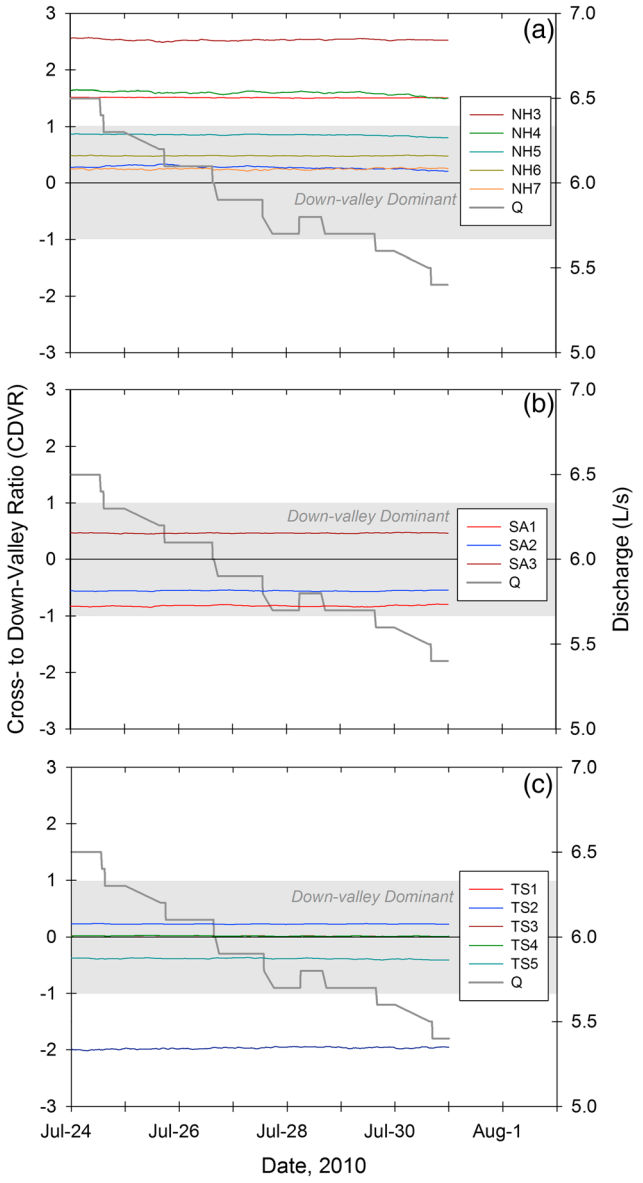

Figure 12. WS01 cross- to down-valley hydraulic gradient ratio (CDVR) for the period from 24 to 31 July when stream flow demonstrated a pronounced diurnal fluctuation due to evapotranspiration within the catchment, for (a) the near hillslope zone, (b) the stream adjacent zone, and (c) the through stream zone. Tick marks are displayed at 00:00 on the day labeled.

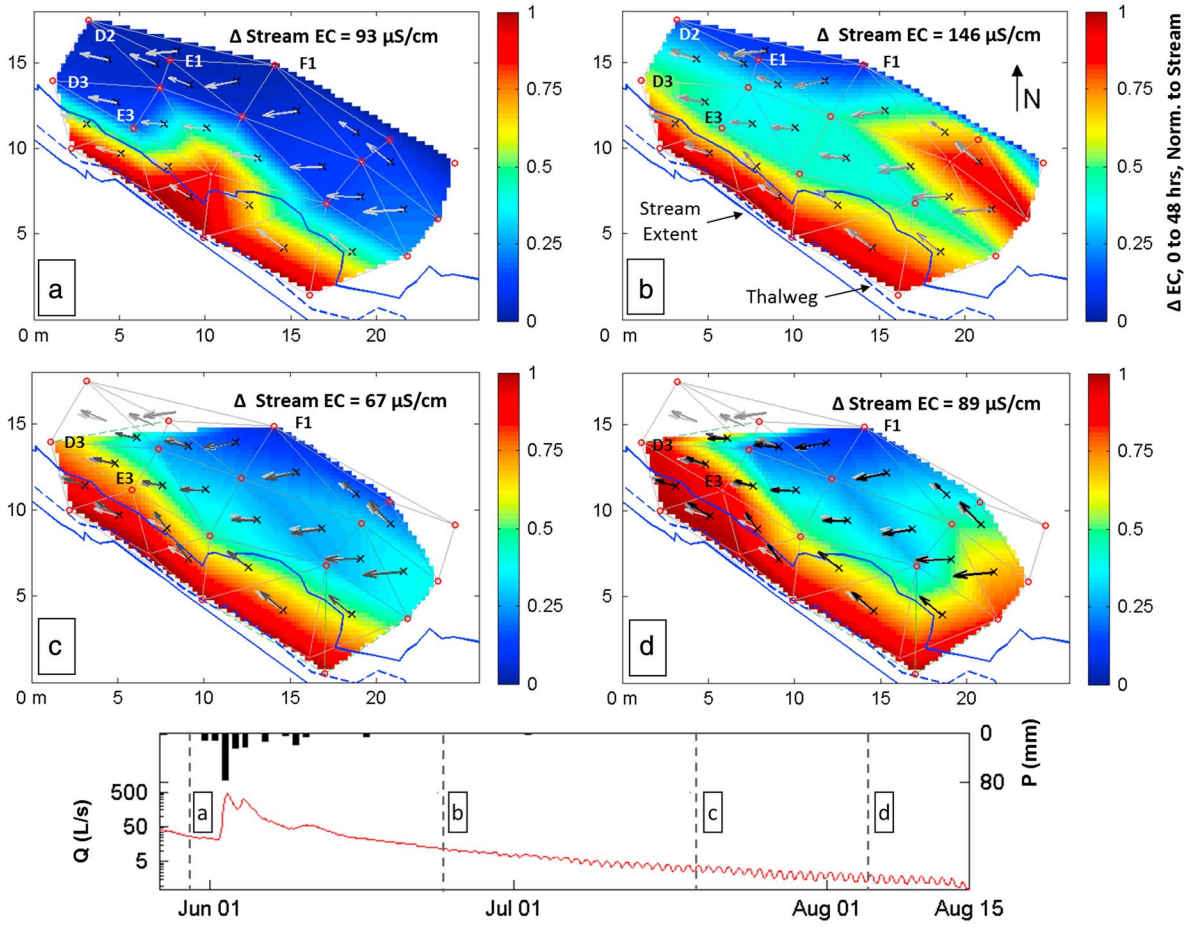

Figure 13. Change in EC in the WS01 riparian zone from 0th to 48th h of four 48 h constant-rate salt tracer injections, normalized to the change in stream EC, set to 1. Gradients at each time step are displayed as arrows that grow darker in color and stack above the earlier arrows as time advances. The colored area diminishes in size as less data becomes available due to wells drying out. The salt tracer was injected about 40 m above the upstream-most well transect. Flow is from bottom right to top left. Hydrograph (Q) in red and hyetograph (P) in black are presented in the bottom panel.

(Figures 13b and 13c) could possibly be an artifact of the particularly high increase in in-stream EC achieved during injection 2, compared to the other three injections.

4.4.2. WS03

[30] Across the narrow riparian zone of WS03, the general pattern of stream water penetration did not change greatly through baseflow recession (Figure 14), although some interesting changes did occur. A few locations showed increased penetration of salt with each injection as the season advances, while still more showed a decrease. Wells D3, E5, and H5 all showed markedly lower EC changes than the rest of the riparian well network during the first two tracer injections, but by the third injection the salty water completely broke through into well D3 and penetrated further into well E5. In contrast, well H5 showed a decrease in relative EC change (from about 0.65 to 0.4) between the first two and last two injections. Similarly, smaller, more gradual decreases in relative EC change were seen in wells I5, H6, G6, and E6 from the earlier to the later injections. While it is difficult to attribute any of these changes to the changes observed in hydraulic gradient direction throughout the season, the lessening intrusion seen around riparian wells G6, G5, and E6 may have been a consequence of the gradients in elements SA1 and SA2 growing weaker and turning towards the stream, which is likely due to the change in stream stage acting as a boundary condition to these elements. On the other hand, well E5 was directly down-gradient (see gradients NH1 and NH3) of the progressively less-impacted well E6, and gradually showed more intrusion of the salt tracer. Given the valley constraints in the cross-valley direction (two–three times as narrow as the WS01 riparian area), it is difficult to identify the extent to which stream water exchanges along the cross-valley axis. However, there is a hint of a boundary to the zone of exchange, in that well G6 showed a progressively declining EC change. This value remained above 0.5 (i.e., 50% "influence" of the stream water) up to the last injection, and was the lowest with the exception of H5, which showed anomalously low EC changes in the latter two injections, possibly due to a more direct connection with non-labeled groundwater that was tempered by the influence of stream water under higher flow conditions. Considering that wells were placed across almost the entire lateral expanse of the valley bottom, and that beyond the wells most distant from the stream were very steep hillslopes, a greater part of the WS03 valley bottom riparian area (in the studied reach) is

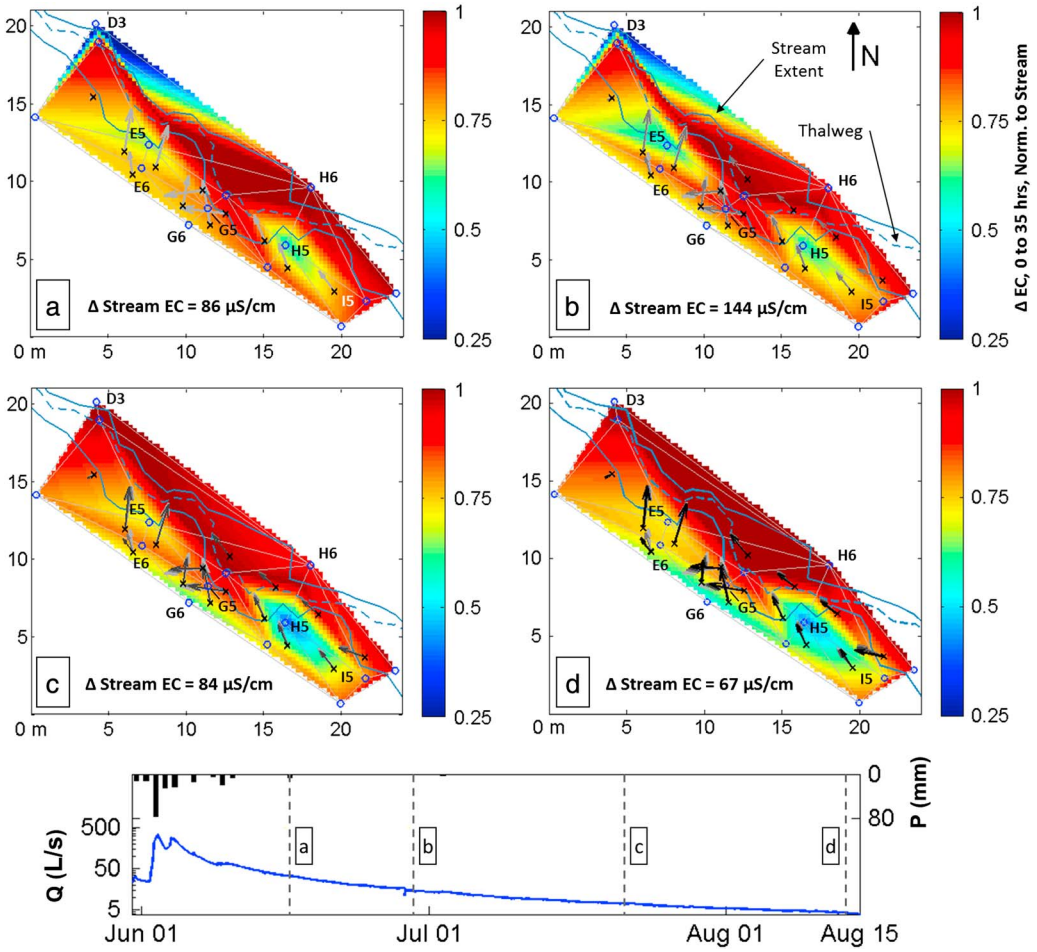

Figure 14. Change in EC in the WS03 riparian zone from 0th to 35th h of four 48 h constant-rate salt tracer injections, normalized to the change in stream EC, set to 1. Gradients at each time step are displayed as arrows that grow darker in color and stack above the earlier arrows as time advances. Blue circles denote wells. The salt tracer was injected about 40 m above the upstream-most well transect. Note that the color bar axis limits are from 0.25 to 1, unlike those in Figure 8 for WS01. Flow is from bottom right to top left. Hydrograph (Q) in blue and hyetograph (P) in black are presented in the bottom panel.

well-connected with the stream, compared to WS01, as would be expected. Because this area is closest to both the saturated zone and the actively flowing stream, this result has implications for biogeochemical cycling in this and other similar systems with narrow and constrained valley bottoms.

5. Discussion

5.1. Riparian Water Tables Did Not Develop Strong Stream-Ward Gradients

[31] Although less prevalent in WS03, both riparian aquifers exhibited down-valley dominance in hydraulic gradients over the entire baseflow recession period (June–August). Gradients throughout the WS01 riparian zone showed strong down-valley dominance, particularly in the stream-adjacent (SA) and middle-riparian (MR) zones. Seasonal trends of note observed in WS01 included the tendency of nearly all gradients in the SA zone—already angled generally away from the stream—to gradually turn even further away from the stream. This is likely due, at least in part, to the stage of the stream channel that is maintained through the summer, acting as a boundary condition to the riparian water table. In addition, two gradients in the more distant near-hillslope (NH) zone began the season angling towards the stream, and ended it angling away.

[32] The seasonal changes observed in WS03 tended to be less pronounced than those in WS01, with a general tendency for all gradients to "straighten out" along the down-valley axis, showing CDVRs that grew closer to zero. However, in absolute terms of CDVR values, WS03 spans a greater range of values, including several strong cross-valley-dominant gradients in the downstream section of the riparian zone, where lateral hillslopes are very steep. There is also an interesting location centered around well G5, where gradients from the NH and SA zones appear to converge strongly on the riparian area downstream of the well, a convergence that grows stronger as the season progresses (Figure 14). This is likely due to a region of fairly high transmissivity located near this well acting as a preferential flow path down-valley. In contrast to WS01, the WS03 valley bottom was subject to considerably more intrusion of salt-labeled water during the tracer injections, although a few locations indicated further intrusion as flow receded throughout the season. The lack of seasonal

variability in stream groundwater exchange compared to gradient changes, indicates that the WS03 valley bottom riparian area is well connected to its stream across a broad range of hydrologic conditions.

[33] The simplified conceptual model of valley-bottom riparian hydrology adjacent to net gaining streams sets the expectation of strong lateral riparian gradients in the direction of the stream (i.e., cross-valley). The resulting expectation is that during times of high baseflow, the zone of stream-groundwater exchange is likely to be limited, or "confined", because the steep lateral subsurface hydraulic gradients would impinge on the channel [*Cardenas and Wilson*, 2007; *Cardenas*, 2009; *Wroblicky et al*., 1998]. Consequently, at low baseflow conditions, we would expect to find a greater potential influence of hydraulic gradients forced by the channel morphology, and greater stream-groundwater exchange, because the lateral water tables would be relatively relaxed. However, this simplified model of subsurface valley-floor hydrology has been found to fail in several cases, as also observed by *Ward et al*. [2012]. For example, in these same headwater valleys in the HJ Andrews Experimental Forest, Oregon, *Wondzell* [2006] conducted stream tracer experiments at high and low baseflow discharges (4.5 and 1 L/s in WS01, and 10 and 3 L/s in WS03, respectively) and reported that the size of the extent of stream water penetration into the riparian zones, as indicated by tracer arrival at wells adjacent to the channel, did not significantly change. This is consistent with the conceptual model put forth by *Larkin and Sharp* [1992], in which the magnitude of cross-valley flow is predicted to be small compared to down-valley flow magnitudes in such steep valleys. Our assessment of both riparian hydraulic gradients and stream water penetration further support the results of *Wondzell* [2006] and *Larkin and Sharp* [1992], and also indicates that the influence of the steep valley slope does not allow for groundwater ridging to occur within the riparian zones.

5.2. Riparian Water Tables Respond Similarly to Storm and Baseflow Recession

[34] Both study areas showed a variety of responses to the 1.25 year storm that took place in early June. The diversity of responses seen in both study areas underlines the heterogeneity inherent on even relatively small spatial scales. In the WS01 near-stream zone, gradients responded to the storm by turning even further away from the stream when the flow peaks passed, suggesting that the storm response drove more stream water into the riparian aquifer. This occurred in spite of most of the more distant gradients turning towards the stream, as conventional conceptual models would suggest. These two results indicate that a trough within the riparian water table formed during the storm, due to a more rapid rise of water table adjacent to this section (i.e., SA and NH), likely due to transmissivity differences within the subsurface. Despite these responses, only one of 23 gradient elements ceased to remain down-valley dominant, and even then only for a brief time, which indicates the dominant influence of the down-valley gradient in the WS01 valley bottom. WS01 exhibited some of the same behavior in response to the storm as it did over the seasonal flow recession, with gradients near the stream turning further away from it, and a number of the more distant ones turning further towards it.

[35] In WS03, the riparian gradients showed a wider variety of more extreme responses to the storm, few of which conformed to conventional ideas. Furthest downstream, two strong cross-valley gradients showed a substantial decline in magnitude in response to the storm. As was observed on the seasonal scale, the converging gradients centered on well E5 converged more intensely during the storm. In the up-valley part of the monitored area, some gradients responded by pointing more weakly towards the stream, while others adhered to conventional conceptual models by showing an enhanced cross-valley component towards the stream.

[36] Hydraulic gradients in WS01 showed noticeable changes in response to the diurnal rise and fall in groundwater levels and stream stage. In the stream-adjacent zone of WS01, at the minimum daily water table elevation, gradients angling towards the stream turned slightly more towards it, and those angled away turned slightly less away. *Wondzell et al*. [2010] proposed a mechanism of lateral hyporheic exchange whereby daily ET-induced drawdown in the riparian water table would draw stream water into the subsurface, sending it back further downstream or later in the day when rising water tables again forced the water back into the stream. The daily-scale CDVRs shown for the stream-adjacent zone in WS01 do not support this as they fluctuate within a range of −1 to 1 (Figure 11).

[37] The complex hydraulic gradient patterns observed throughout the study period for our two sites are similar in character to those observed in past studies both at these same sites and at other headwater sites. Taken as a whole, the hydraulic gradient patterns in our study reflect the overall down-valley dominance seen in the modeled equipotential maps of both study sites [*Kasahara and Wondzell*, 2003], but show some more detail on a small spatial scale not captured by the model, particularly in the strong cross-valley gradients in the lower portion of the monitored WS03 riparian area. Studies at other headwater sites also showed similar down-valley dominance of riparian hydraulic gradients, as well as a variety of more complex gradient dynamics in localized areas within the riparian zones [*Harvey and Bencala*, 1993; *Wroblicky et al*., 1998].

[38] The overall seasonal changes exhibited by gradients in the two small riparian areas studied seem to be relatively small, and overall patterns relatively stable, compared to other systems. For example, a field-based and two-dimensional transient groundwater modeling study of riparian groundwater flow in New Mexico headwater streams during different flow conditions showed a much more dynamic response to changes in flow over a larger scale [*Wroblicky et al*., 1998]. Likely, this was due to the broader and lower gradient valley floor setting (overall), and the transmissivity of the valley floor materials compared to WS01 and WS03. In hillslope-constrained riparian areas of a stream with a catchment area only three times as large as WS01 and WS03, the authors observed and modeled large changes in gradient direction, ranging from about 30° away from the stream during low flow conditions to about 15° towards or parallel to the stream during high spring-melt flow conditions (our interpretation) [*Wroblicky et al*., 1998]. Seasonal water table fluctuations were also as much as an order of magnitude greater than those observed in our study areas. In riparian zones draining much larger catchments, a wide

variety of responses over different flow conditions, ranging from virtually no change to complete reversal of gradient direction has been observed [*Vidon and Hill*, 2004]. This same study found large seasonal fluctuations in water table, as large as 1 to 2 m, while the largest seasonal fall in riparian water level (excluding the storm peaks) seen in WS01 or WS03 was 20 cm, with the average between 10 and 15 cm. This is reflected by the relatively slight changes observed in stream-groundwater exchange.

5.3. Stream-Groundwater Exchange Varied Little Through Baseflow Recession

[39] Several conceptual models of stream-groundwater interaction have been proposed in headwater valley floor settings. In one particular model developed in WS01, *Bond et al*. [2002] predict that near-stream hyporheic flowpaths will diminish (i.e., hyporheic exchange will shrink in spatial extent) as stream flow decreases during baseflow recession. *Wondzell et al*. [2010] address this point with evidence from tracer studies suggesting that there is not an appreciable change in relative dominance of short- versus long-scale hyporheic flow paths as flow recedes. The results of our tracer injections in both watersheds showed relatively slight changes in stream-groundwater exchange. In WS01, we found that more stream-groundwater exchange occurs as flow recedes and the catchment dries (Figure 13), supporting the findings of *Wondzell et al*. [2010]. However, while WS03 showed a more extensive valley-bottom connection between stream and riparian aquifer, there was a slight decrease in the lateral extent of the stream-groundwater exchange through the season. This is possibly due to some locations that become more disconnected from the main tracer-bearing flow, for instance as the water level fell and some locations became blocked by previously submerged large cobbles [*Desilets et al*., 2008]. Our results also support the findings of *Ward et al*. [2012], who used electrical resistivity methods to map hyporheic penetration in two dimensions through time, and noted that hydraulic gradients in WS03 did not inhibit tracer penetration into the riparian aquifer. Together these findings suggest that the hydraulic conductivity field of the riparian aquifer is a strong control on stream water movement through this zone.

[40] With regard to the extent of stream water intrusion into the riparian zones of WS01 and WS03, which is one indicator of the size of the stream water exchange zone, it is difficult to make substantive judgments about this area without a firm definition of where along the cross-valley axis to draw the line between the areas that are or are not connected to the stream. *Triska et al*. [1989] propose that a location in the aquifer is influenced by the stream if it receives greater than 10% of the tracer-labeled stream water. By this definition, both headwater riparian zones in this study are extraordinarily well connected to the stream, having stream-influenced areas that span essentially the entire valley bottom of both watersheds (except WS01 during the first injection, where only about half of the valley bottom showed $> 10\%$ stream water), up to where the very steep ($> 50\%$ slope), confining hillslopes begin, beyond which we have no information. Indeed, the only limitation to hyporheic area in these locations appears to be the width of the valley bottom, and more extensive field investigations would need to be undertaken to establish at which point on the lower hillslope the break occurs between pure groundwater and groundwater in connection with the surface stream water. Furthermore, the seasonal patterns evident in the changing extent of stream water intrusion into the riparian zone, particularly in WS01, are in agreement with a few studies, which find that the stream-groundwater exchange areas of the riparian aquifers are augmented when flows are lowest [*Valett et al*., 1997; *Wroblicky et al*., 1998], but disagreed with others [e.g., *Fraser and Williams*, 1998].

[41] While the seasonal trend (especially in WS01) indicates a correlation between lower flows (and an overall drier catchment) and increased stream-groundwater exchange, it is important to draw attention to the observation that the response of near-stream riparian gradients to the storm mirrored that of their response to the seasonal flow recession. The apparent increase in stream-groundwater interaction is directly linked to the seasonal patterns observed in the near-stream hydraulic gradients throughout the baseflow recession period. It is therefore likely that the (albeit relatively short-lived) gradient patterns during the storm would elicit a similar change in the extent of stream-groundwater interaction.

6. Conclusions

[42] The primary objectives of this study were to investigate how water table gradients in headwater valleys change in response to different hydrological forcings, determine how the temporal dynamics of the water table compare to riparian topographic gradients, and assess with the help of tracer studies how these water table dynamics impact stream-groundwater interaction. We conclude that, with respect to patterns in hydraulic gradients and potential for stream-groundwater exchange, although less pronounced in WS03, both WS01 and WS03 turned away from the stream during seasonal declines in flow. In WS01, near-stream gradients gradually turned away from the stream, while most other gradients gradually turned towards the stream. In WS03, there was a general tendency for hydraulic gradients to turn towards the down-valley axis, pointing more dominantly downstream as the season progressed. Relative to other studies in headwater valleys, the seasonal responses observed in both watersheds are relatively stable, but dominated by a persistent overall down-valley gradient. Both watersheds exhibited changes in the extent of intrusion of salt-labeled stream water into the riparian zones in response to the constant-rate tracer injections as the season progressed and flows receded. In WS01, there was a relatively steady increase over the season in the penetration of salt-labeled stream water into the riparian aquifer (eight of 11 wells had $\geq 30\%$ stream water by the last injection). This is expected, given the observation of the near-stream hydraulic gradients' seasonal tendency to turn away from the stream, which is driven by the stream stage acting as a boundary condition for the stream-adjacent elements of the water table. In WS03, a net seasonal decrease in stream water intrusion was slight, although nearly the entire valley bottom aquifer was penetrated by $> 50\%$ stream water for all injections. Thus, despite the changing hydraulic gradients, connection between streams and valley floor aquifers was strong.

[43] In response to a 1.25 year storm event, WS01 riparian hydraulic gradients exhibited similar behavior to that observed across the entire season, pointing to the potential for storms to drive increased stream-groundwater exchange. With a minor exception, all hydraulic gradients in WS01 were down-valley dominant, even at the peak of the storm, implying that subsurface travel times of stream water could remain long, even during a storm. WS03 riparian hydraulic gradients showed a more diverse set of responses, few of which reflected conventional ideas about cross-valley-dominated flow during storms. For example, one area exhibited a sharp decline in total hydraulic gradient magnitude, while another area showed a strong potential for convergence of flow on one riparian location. Daily water table fluctuations produced diurnally varying cross- to down-valley hydraulic gradient ratios in WS01, while no response was observed in WS03. These results indicate that, over a broad range of hydrologic conditions, streams and riparian aquifers of steep headwater valleys are tightly connected and that the steep longitudinal gradient of the valley floors is a reasonable predictor of a flow-independent dominant riparian flow direction.

[44] **Acknowledgments.** The authors would like to gratefully acknowledge the field support provided by the HJ Andrews Experimental Forest staff and scientists, and the review comments of J. Buffington (AE) and three anonymous reviewers. This research was supported by the National Science Foundation, grant EAR 09-11435. Any opinions, findings, and conclusions, or recommendations expressed in this material are those of the authors and do not necessarily reflect the views of the National Science Foundation.

References

Bond, B. J., J. A. Jones, G. Moore, N. Phillips, D. Post, and J. J. McDonnell (2002), The zone of vegetation influence on baseflow revealed by diel patterns of streamflow and vegetation water use in a headwater basin, *Hydrol. Proc.*, *16*, 1671–1677.

Burt, T. P., L. S. Matchett, K. W. T. Goulding, C. P. Webster, and N. E. Haycock (1999), Denitrification in riparian buffer zones: The role of floodplain hydrology, *Hydrol. Proc.*, *13*, 1451–1463.

Burt, T. P., et al. (2002), Water table fluctuations in the riparian zone: Comparative results from a pan-European experiment, *J. Hydrol.*, *265*(1–4), 129–148.

Burt, T., M. M. Hefting, G. Pinay, and S. Sabater (2008), The role of floodplains in mitigating diffuse nitrate pollution, in *Hydroecology and Ecohydrology: Past, Present and Future*, edited by P. J. Wood, D. M. Hannah, and J. P. Sadler, John Wiley & Sons, Ltd, Chichester, UK, doi:10.1002/9780470010198.ch14.

Cardenas, M. B. (2009) Stream-aquifer interactions and hyporheic exchange in gaining and losing sinuous streams, *Water Resour. Res.*, *45*, W06429, doi:10.1029/2008WR007651.

Cardenas, M. B., and J. L. Wilson (2007), Exchange across a sediment-water interface with ambient groundwater discharge, *J. Hydrol.*, *346*(3–4), 69–80, doi:10.1016/j.jhydrol.2007.08.01.

Cirmo, C. P., and J. J. McDonnell (1997), Linking the hydrologic and biogeochemical controls of nitrogen transport in near-stream zones of temperate-forested catchments: A review, *J. Hydrol.*, *199*(1–2), 88–120, doi:10.1016/S0022-1694(96)03286-6.

Covino, T., B. McGlynn, and J. Mallard (2011), Stream-groundwater exchange and hydrologic turnover at the network scale, *Water Resour. Res.*, *47*, W12521, doi:10.1029/2011WR010942.

Desilets, S. L. E., T. P. A. Ferre′, and P. A. Troch (2008), Effects of stream-aquifer disconnection on local flow patterns, *Water Resour. Res.*, *44*, W09501, doi:10.1029/2007WR006782.

Dunne, T., and R. D. Black (1970), An experimental investigation of runoff production in permeable soils, *Water Resour. Res.*, *6*(2), 478–490.

Duval, T. P., and A. R. Hill (2006), Influence of stream bank seepage during low-flow conditions on riparian zone hydrology, *Water Resour. Res.*, *42*, W10425, doi:10.1029/2006WR004861.

Dyrness, C. T. (1969), Hydrologic properties of soils on three small watersheds in the western Cascades of Oregon, *Res. Note PNW-111*, Pac. Northwest For. and Range Exp. Stn., For. Serv., U.S. Dep. of Agric., Portland, Oreg.

Fraser, B. G., and D. D. Williams (1998), Seasonal boundary dynamics of a groundwater/surface-water ecotone, *Ecology*, *79*(6), 2019–2031.

Gillham, R. W. (1984), The capillary fringe and its effect on water-table response, *J. Hydrol.*, *67*, 307–324.

Groffman, P. M., G. Howard, A. J. Gold, and W. M. Nelson (1996), Microbial nitrate processing in shallow groundwater in a riparian forest, *J. Environ. Qual.*, *25*(6), 1309–1316.

Harvey, J. W., and K. E. Bencala (1993), The effect of streambed topography on surface-subsurface water exchange in mountain catchments, *Water Resour. Res.*, *29*(1), 89–98.

Jencso, K. G., B. L. McGlynn, M. N. Gooseff, S. M. Wondzell, K. E. Bencala, and L. A. Marshall (2009) Hydrologic connectivity between landscapes and streams: Transferring reach and plot scale understanding to the catchment scale, *Water Resour. Res.*, *45*, W04428, doi:10.1029/2008WR007225.

Kasahara, T., and S. M. Wondzell (2003), Geomorphic controls on hyporheic exchange flow in mountain streams, *Water Resour. Res.*, *39*(1), 1005, doi:10.1029/2002WR001386.

Larkin, R. G., and J. M. Sharp, Jr. (1992), On the relationship between river-basin geomorphology, aquifer hydraulics, and ground-water flow direction in alluvial aquifers, *GSA Bull.*, *104*, 1608–1620.

Payn, R. A., M. N. Gooseff, B. L. McGlynn, K. B. Bencala, and S. M. Wondzell (2009), Channel water balance and exchange with subsurface flow along a mountain headwater stream in Montana, United States, *Water Resour. Res.*, *45*, W11427, doi:10.1029/2008WR007644.

Rothacher, J., C. T. Dyrness, and R. L. Fredriksen (1967), Hydrologic and related characteristics of three small watersheds in the Oregon Cascades, report, Pac. Northwest For. and Range Exp. Stn., For. Serv., U.S. Dept. of Agric., Portland, Oregon.

Sklash, M. G., and R. N. Farvolden (1979), The role of groundwater in storm runoff, *J. Hydrol.*, *43*, 45–65.

Sophocleous, M. (2002), Interactions between groundwater and surface water: The state of the science, *Hydrogeol. J.*, *10*(1), 52–67.

Swanson, F. J., and M. E. James (1975), Geology and geomorphology of the H.J. Andrews Experimental Forest, western Cascades, Oregon, *Res. Pap. PNW-188*, Pac. Northwest For. and Range Exp. Stn., For. Serv., U.S. Dep. of Agric., Portland, Oreg.

Swanson, F. J., and J. A. Jones (2002), Geomorphology and hydrology of the H.J. Andrews Experimental Forest, Blue River, Oregon, *Field Guide to Geologic Processes in Cascadia*: *Oregon Department of Geology and Mineral Industries Special Paper 36*, 289–314.

Triska, F. J., V. C. Kennedy, R. J. Avanzino, G. W. Zellweger, and K. E. Bencala (1989), Retention and transport of nutrients in a third-order stream in northwestern California: Hyporheic processes, *Ecology*, *70*(6), 1893–1905.

Valett, H. C., C. N. Dahm, M. E. Campana, J. A. Morrice, M. A. Baker, C. S. Fellows (1997), Hydrologic influences on groundwater-surface water ecotones: Heterogeneity in nutrient composition and retention, *J. N. Am. Benthol. Soc.*, *16*(1), 239–247.

Vidon, P. G. F., and A. R. Hill (2004), Landscape controls on the hydrology of stream riparian zones, *J. Hydrol.*, *292*, 210–228.

Ward, A. S., M. Fitzgerald, M. N. Gooseff, T. J. Voltz, A. M. Binley, K. Singha (2012), Hydrologic and geomorphic controls on hyporheic exchange during baseflow recession in a headwater mountain stream, *Water Resour. Res.*, *48*, W04513, doi:10.1029/2011WR011461.

Winter, T. C. (2001), The concept of hydrological landscapes. *J. Am. Water Resour. Assoc.*, *37*, 335–349, doi:10.1111/j.1752-1688.2001.tb00973.x.

Woessner, W. W. (2000), Stream and fluvial plain ground water interactions: Rescaling hydrogeologic thought, *Ground Water*, *38*(3), 423–429.

Wondzell, S. M. (2006), Effect of morphology and discharge on hyporheic exchange flows in two small streams in the Cascade Mountains of Oregon, USA, *Hydrol. Processes*, *20*, 267–287.

Wondzell, S. M., M. N. Gooseff, and B. L. McGlynn (2010), An analysis of alternative conceptual models relating hyporheic exchange flow to diel fluctuations in discharge during baseflow recession, *Hydrol. Proc.*, *24*, 686–694, doi:10.1002/hyp.7507.

Wroblicky, G. J., M. E. Campana, H. M. Valett, and C. N. Dahm (1998), Seasonal variation in surface-subsurface water exchange and lateral hyporheic area of two stream-aquifer systems, *Water Resour. Res.*, *34*(3), 317–328.